
Article:
Li, P., Batey, D. and Rodenburg, J. (2019) An X-ray ptycho-tomography model of 'Seeing order in "amorphous" materials'. Ultramicroscopy. ISSN 0304-3991

https://doi.org/10.1016/j.ultramic.2019.02.006

An X-ray ptycho-tomography model of 'Seeing order in "amorphous" materials'

Peng Li[1], Darren Batey[2] and John Rodenburg*

Department of Electronics and Electrical Engineering, University of Sheffield, S1 3JD, UK

[1]Current address: Aix-Marseille University, CNRS, Institut Fresnel, 13013 Marseille, France.

[2]Current address: Diamond Light Source, Harwell Science and Innovation Campus, Fermi Ave, Didcot OX11 0DE, UK

*Corresponding author, email: J.M.Rodenburg@shef.ac.uk

Abstract:

The nature of the atomic structure of many non-crystalline materials remains a long-standing open question. We use X-ray scattering to model electron images of amorphous materials, where the analogue 'atoms' consist of 1μm diameter glass beads. The beads form a substantially random close-packed structure, but are partially ordered in places. X-ray ptycho-tomography reveals the exact position of the beads in 3D and so can be used to compare the modelled electron image with full knowledge of the underlying real structure. Using this, we repeat an experiment reported by Archie Howie and colleagues in 1978 that sought to test for real structure in bright-field electron images of amorphous materials; we demonstrate the validity of the technique, at least in the case of the resolution of the microscopes available at that time and the first Born approximation. We also illustrate how extremely demanding it would have been to infer 3D structure of amorphous material from pairs of stereoscopic images obtained with the same experimental kit: an approach that Archie proposed in the 1970s. We briefly discuss the possibility of using electron ptycho-tomography to solve the amorphous structure problem.

KEYWORDS: Amorphous, Non-Crystalline, Ptychography, Electron imaging, Ptycho-tomography, X-ray imaging

1) Introduction:

This special issue of Ultramicroscopy is dedicated in part to the celebration of the 85th birthday of Archie Howie. We therefore thought it might be interesting to revisit a subject that he worked on and has discussed in a number of papers over the last 40 years: the question of how electron microscopy might unravel the mystery of the structure of amorphous materials (for reviews, see [1, 2]). The study of metallic crystals – and in particular faults within them – dominated much of the early history of electron microscopy, at least as it applied to materials science. Of course, this was an integral part of Archie's early work in Hirsch's group, leading to the famous book *'Electron microscopy of thin crystals'*, otherwise known by some of us older electron microscopists as 'The Bible' [3]. However, as lens design of the transmission electron microscope (TEM) improved, approaching a resolution of 3Å or so, the observation of bright-field images of amorphous or non-crystalline specimens, such as amorphous carbon (a-C), amorphous Ge (a-Ge), and amorphous silica, became routine.

These specimens result in random (or pseudo-random) bright-field images, and contain no obvious long-range order. They are speckled and often contain contiguous patches of fringes, some of which look tantalisingly like highly distorted Bragg planes (sometimes referred to as 'quasi Bragg planes' [4, 5]). For the purposes of this paper, we will call this type of contrast 'fringy', emphasising the fact that the eye often does perceive layering in the contrast, whether or not this is real structure or an optical illusion. When these images were first obtained, there was great hope that the structure of non-crystalline materials might be deciphered by the electron microscope: an explicit description of the structure of non-crystalline or amorphous materials remains to this day an open question. In particular, the fringy structure implied that there might be micro- or nano-crystallites imbedded in an otherwise amorphous structure, or that some sort of other medium range order was being expressed in the image.

When used as a support film, a-C nowadays appears in almost any atomic resolution image of small particles. Indeed, most aberration corrected electron microscopes rely on amorphous material – even if only amorphous contamination – to align their optics. A random amorphous structure provides a wide and continuous spectrum of Fourier components, thus allowing the diffractograms of a series of bright-field images to measure accurately zeros in the contrast transfer properties of the lens, including residual errors that require correction. Similar measurements can be made via the Ronchigram using an amorphous film.

The study of amorphous materials is a massive field of research that we make no attempt to review here: the reader will find plenty of textbooks on the subject. Suffice it to say that at one extreme of order we have the perfect crystal, while at the other extreme we can imagine we have a 'maximally disordered' arrangement of atoms. Total disorder in the solid state, in the sense that the atomic coordinates are distributed perfectly randomly, is impossible if only because of packing constraints. Depending on their ionisation state, atoms have quite well determined diameters. If they behave as solid spheres (i.e. without

preferred bonding configurations), then any two atoms cannot be closer to one another than their combined radii. Even if we somehow force the atoms pack as randomly as possible (say – in the case of metals – via extreme quenching rates and/or by choosing a complicated stoichiometry), only a certain number of atoms can fit around any particular atom, determining a shell structure with an associated approximate coordination number. Atoms yet further away from a particular atom will still be somewhat constrained in their positions, forming a second shell, albeit of less distinct structure. These shells mean that there are still, on average, more or less prevalent separations between the atoms, and this in turn gives rise to broad rings in the diffraction pattern. For a material like silica glass (amorphous SiO_2), bonding angles are also constrained (unlike in the hard sphere model). The silicon resides at the centre of a tetrahedral unit of oxygen atoms, in the same local environment as it is found in the crystalline form of silica. The glassy state arises from randomised rings of different numbers of tetrahedra connected at their vertices by the oxygen atoms.

However, the conventional diffraction pattern averages bond length information from a macroscopic sample. Other spectroscopic methods can yield very local bonding information, but again averaged over all the bonds in the volume illuminated by the probing radiation (which admittedly can be very small in a modern scanning transmission electron microscope). We can conjecture that a material that appears amorphous in any such averaged measurement in fact has local structure over distances much larger than those determined by the 'maximally' disordered constraints discussed above. For example, we might postulate that there are nano-crystallites imbedded in an otherwise random structure, or that the majority of the structure is composed of nano-crystallites, which are each extremely distorted because of the high volume ratio of material dominated by grain boundary forces.

Back in the 1970s, the question arose: do these fringy images of amorphous materials imply that amorphous material are actually more ordered than a purely 'maximally random' structure? In particular, fringes sometimes appear in clusters, approximately parallel with one another. Is this real structure or just chance statistics? We can further divide the issue into three subsidiary questions.

(i) We know the bright-field imaging mechanism is wholly dependent on the contrast transfer function (CTF) of the objective lens, and so it is possible that the statistical nature of fringy images arises simply from the limitations (zeros and contrast reversals) of the transfer function itself, and bears no relationship whatsoever to the underlying atomic structure of the object.

(ii) Perhaps the fringy structure does indeed arise from real structure in the specimen. Layers of graphitised carbon clearly show strong order – enough to use the graphitised layers (when seen edge on) as a standard resolution test specimen. It would seem logical to suppose that partially crystalline regions within the specimen may cause the much less ordered fringy images seen in ordinary sheets of a-C, or other amorphous materials. Indeed, even very

disordered models can show fringy structure, or pseudo Bragg planes, when seen from particular orientations [6].

(iii) Conversely, perhaps the specimen contains significant local periodic or other systematic structure, but that this structure is obliterated by the nature of the imaging process. The biggest single challenge in hoping to see order in a 'thick' specimen is the projection effect (where 'thick 'means anything thicker than a few tens of Angstroms – in practice extremely thin). Atoms on the top, middle and the bottom of the object appear to be in the same x-y plane of the image, and so even if there is a very ordered region somewhere within the depth of the object, its structure will be overwhelmed by chance overlaps with atoms above or below it that have no relationship whatsoever with the ordered region.

In this paper we present an X-ray analogue of the amorphous material atomic resolution bright-field electron-imaging problem. The advantage of using X-rays is that we can perform the experiment on a much larger scale, and by using ptycho-tomography [7] determine the exact position of all the 'atoms' in the specimen (modelled by 1μm diameter glass beads). The advantage of using a real scattering experiment like this, instead of modelling the whole experiment in a computer, is that generating a pseudo-ordered specimen is difficult, whereas in the present case our glass bead structure naturally forms regions of pseudo-crystallinity and volumes of truly disordered, close-packed structure. As is usual in any type of ptychography [8, 9], we recover each projection of the object as a complex image (i.e. with real and imaginary components) and so we can use this to simulate the exit wave in a conventional TEM and hence calculate the bright-field image.

In particular, we repeat an experiment reported in Nature by Ondrej Krivanek, Phil Gaskell and Archie Howie (which we refer to as KGH) with the title, "Seeing order in 'amorphous' materials"[10]. With access to the full tomographic data of our model material, we can demonstrate visually how exceedingly demanding – in fact impossible – it is to retrieve any meaningful information from any one single electron micrograph. In a review written in 1978 [1], Archie suggested that a stereoscopic approach might mitigate the projection effect. We find that, at least for a very thin specimen, it is possible to see 3D effects from two stereoscopic images of an amorphous structure, even with a microscope with the low resolution available in 1978, but not in a way that is very meaningful. What is clear, however, is that a tomographic set of fringy amorphous images recorded in phase, say via ptychography, do indeed contain all the structural information in the object, if indeed we are able to tilt the specimen through a full tomographic series of projection angles.

What we do not have space to discuss, or even review, is the enormous amount of work that has since been done on different statistical signals available in the electron microscope (other than the bright-field image) that can detect other measures of order in highly-disordered materials. Perhaps the most important class of these techniques is fluctuation microscopy [11] pioneered by Treacy, Gibson and Voyles (see for example [12, 13]), and which has generated a very

active field of research. In principle, our X-ray model could be used to assess such techniques, but that will have to be the subject of further work.

2) Experimental:

We manufacture two pseudo-amorphous objects consisting of 1μm diameter glass beads. One specimen is assembled in a glass capillary tube of inner diameter 42μm, the other in a tube of inner diameter 117μm diameter. The two specimens were used to undertake the first tests of X-ray ptycho-tomography at the Diamond Light Source in 2015, but the data can act as a useful model in the current work. We took no particular care in packing the glass beads, but simply dipped the capillary into a water suspension of the beads, which were then naturally drawn up by the capillary force, and then left to dry. The tubes were mounted vertically and illuminated by a focussed beam of 9.12keV X-rays at the I13 beamline at the Diamond Light Source, as illustrated in Figure 1. A coherent area of the beam was selected by apertures upstream of a Fresnel zone plate (FZP) lens. A circular beam footprint with a diameter of 8.75μm was produced on the specimen as a result of placing the specimen slightly upstream of the FZP focus. The transmitted diffraction patterns were collected by an area detector (composed of 2×2 arrays of MediPix3 chips each with 512×512 pixels of 55μm ×55μm) and it was positioned 7.284m downstream of the sample. The specimen was rotated around 180 degrees in one degree steps for the 42μm tube and in 0.5 degree steps for the 117μm tube. Under each orientation, in the plane perpendicular to the beam propagation direction, the specimen was scanned over a 12×26 position grids for the 42μm tube and 12×70 for the 117μm tube with a nominal step size of 2.5μm plus ±20% random offsets. The exposure time of the detector at each scan position was 0.25s for the 42μm tube and 0.15s for the 117μm tube. The ePIE [14] algorithm was used to reconstruct the object images for all the orientations. The phase parts of these object images were then used to construct the tomograph using standard back projection methods. Further details of the experimental procedures and parameters, together with the data processing methods, can be found in the on-line thesis of Li [15]. The X-ray ptycho-tomographic reconstruction was obtained for each specimen in such a way that the wavelength of the radiation and the scattering angles detected mimicked those that could be obtained in a scanning transmission electron microscope (STEM), wherein the 1μm beads would scale equivalently with size of atoms of diameter of 2-3Å. (The exact scaling was dependent on modelling graphite fringes – see below.)

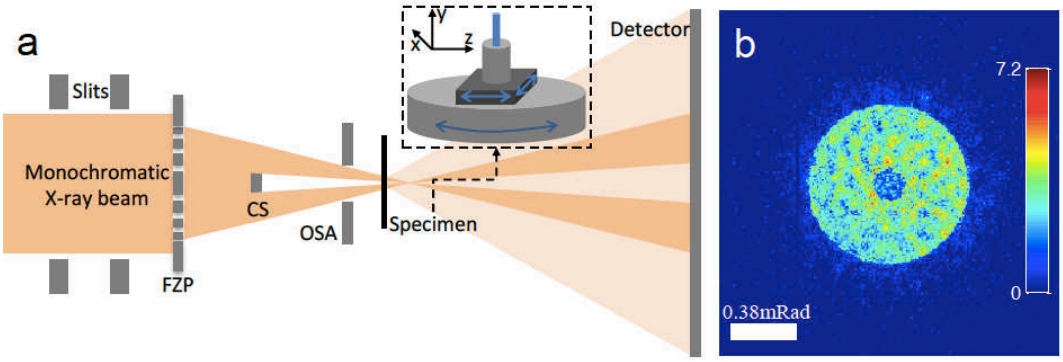

Figure 1) (a) Schematic of the experimental set up. The capillary tube containing the glass beads is mounted vertically on an x-y stage that can be rotated on axis. A high brightness X-ray beamline provides a coherent flux of X-rays that are focussed by a Fresnel zone lens onto the specimen. The specimen is mounted a small distance from the focal length of the lens so as to increase the spot size. Scattered photons are recorded in the Fraunhofer diffraction plane. (b) Example of the raw data on the detector.

Figure 2 shows the phase image of the transmission function of one projection from the 117μm specimen. We display phase because the modulus of the specimen transmission at this energy is approximately unity (no absorption), and we will use this signal to model the electron bright-field image, where a similar phase specimen approximation applies. Figures 3 and 4 show partial cross-sections through the two ptycho-tomographic reconstructions. We see that, especially in the narrower tube, there are quite significant volumes in which the glass beads stack in a pseudo-crystalline way, although in the majority of the volume the stacking is random. The specimens therefore represent amorphous materials that contain some localised volumes of order. The stripy radial contrast at the tube wall in figure 4b is caused by the angular sampling in the measurements (i.e. a small degree of angular undersampling [16]). Note that some glass beads appear darker in contrast: this is because the cross-section of the reconstruction has passed through the top or bottom cross-section of the individual bead.

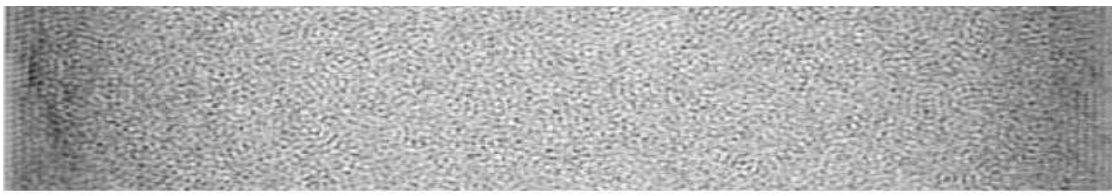

Figure 2: Phase component of the ptychographic image recorded for one projection from the 117μm tube (the full field diameter is shown). Note that the image is remarkably reminiscent of fringy amorphous images obtained in the TEM. Because the specimen is cylindrical, the phase is weaker (darker) at the edges of the field of view.

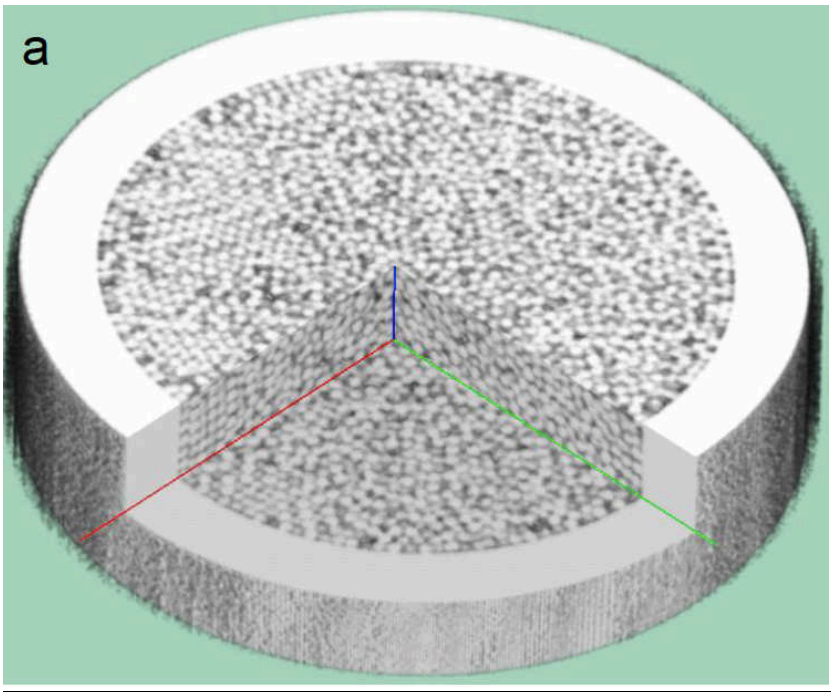

Figure 3: (a) 3D view and cross-section of the 42μm tube tomographic reconstruction of the glass bead structure. Note there are some significant volumes of pseudo-crystalline ordering, particularly noticeable in the left hand quadrant of the tube. The red, green and blue lines correspond to those shown in the cross-sections in Figures 3(b, c and d).

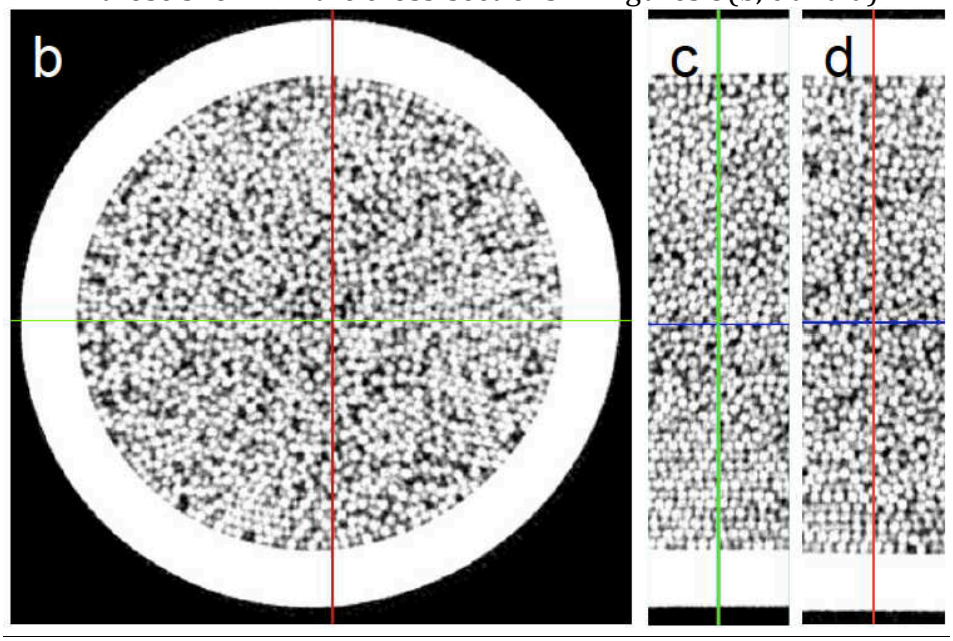

Figure 3b: Cross-sections of the tomographic reconstruction shown in Figure 3a. In (c) and (d) the green and red lines are co-incident in the real object, and show sections at taken parallel with the tube axis.

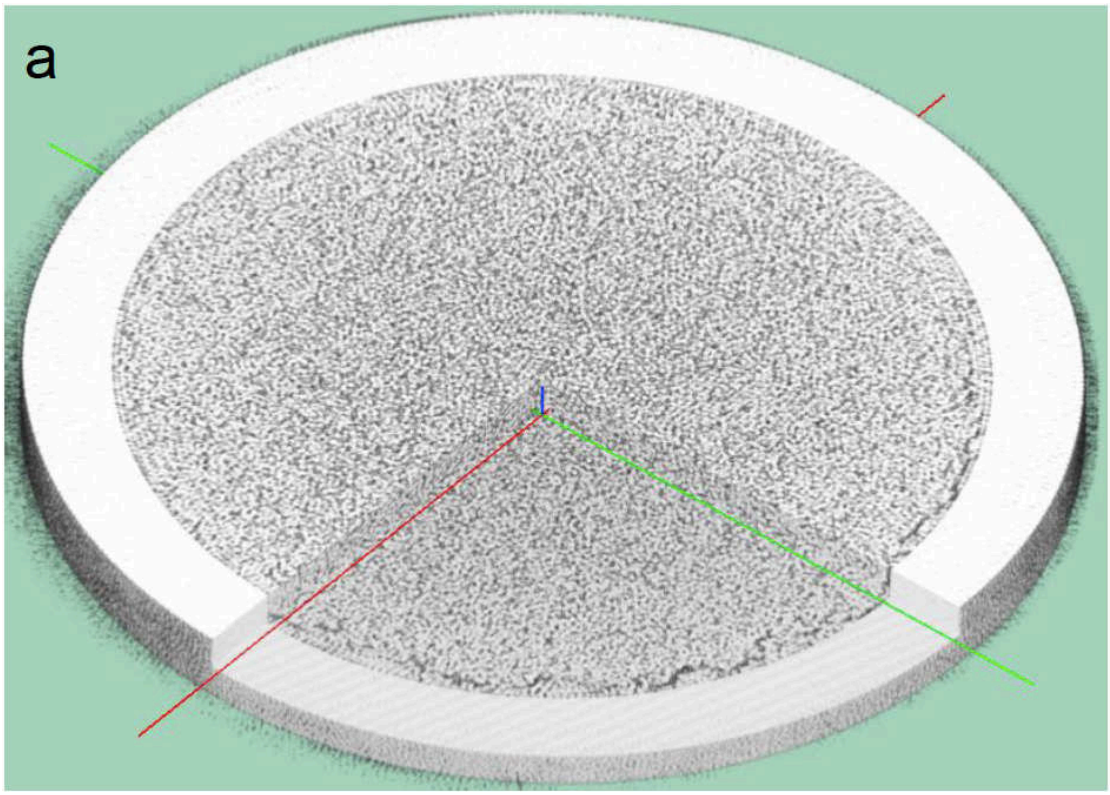

Figure 4a: 3D view and cross-section of the 117μm tube tomographic reconstruction of the glass bead structure. The red, green and blue lines correspond to those shown in the cross-sections in Figures 4(b, c and d).

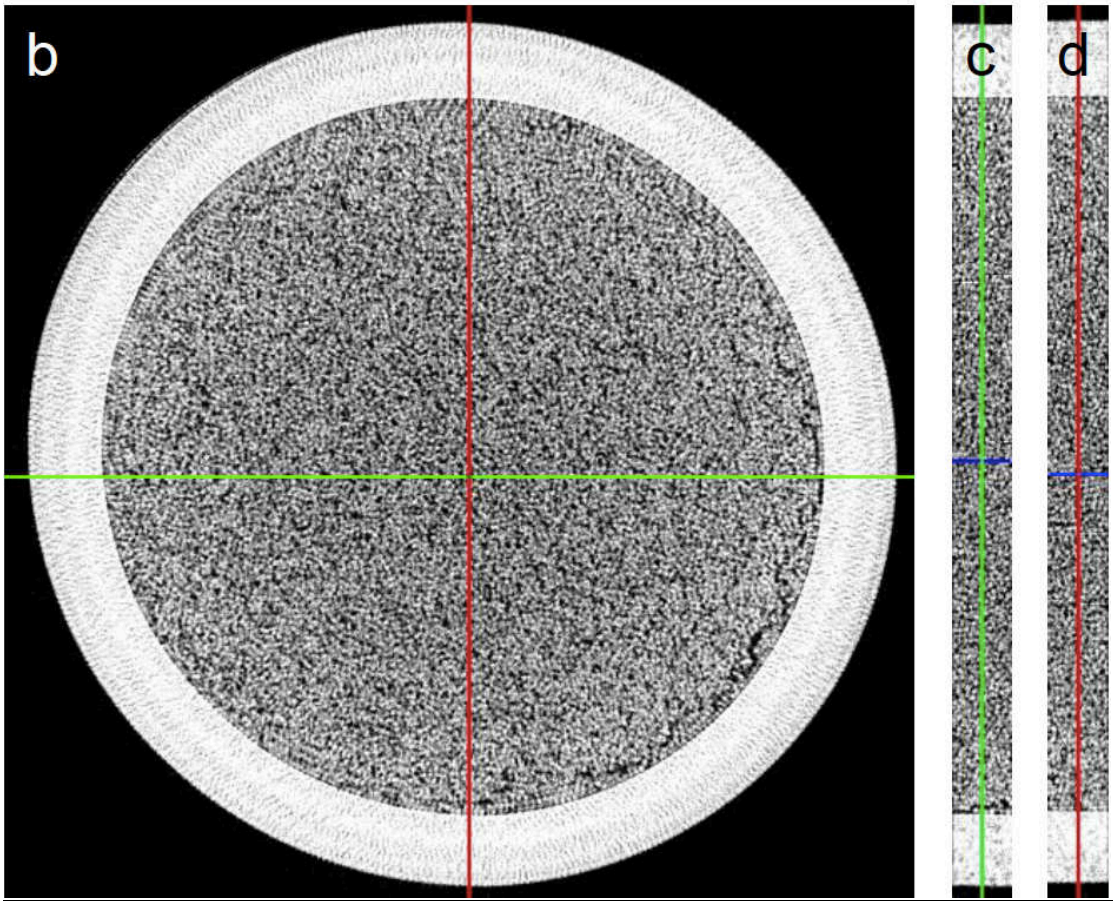

Figure 4b: Cross-sections of the tomographic reconstruction shown in Figure 4a. . In (c) and (d) the green and red lines are co-incident in the real object, and show sections at taken parallel with the tube axis.

3) Seeing order in 'amorphous' materials

The phase of an X-ray ptychograph is a projection of the optical potential integrated along the line of sight, perpendicular to the image plane [7]. The fringes we see in Figure 2 therefore arise directly from the distribution of glass beads, with larger phase corresponding regions where there is a greater than average number of beads lined up along the line of sight. These fringes are the only information that contributes to the tomographic reconstruction, which itself relies on the linear projection approximation. Reversing the argument, we can say that the fact that we get a good tomographic reconstruction, with well-isolated glass beads visible, implies that indeed the fringes in each individual projected image are wholly determined by the projected positions of beads.

In the bright-field electron image, there is a contrast transfer function that will miss out some periodicities in the image and reverse the contrast of others. However, we will see below that the overwhelming structure in both the phase of the ptychograph (Figures 5a and 7a), and the corresponding simulated bright field images that we generate from this data (Figures 5b and 7b), is the fringy structure, which we know arises from the actual position of the glass beads. We can infer that the real fringy images encountered in electron microscopy are not

simply a random consequence of the imaging technique *per se*: they are principally determined by the exact atomic positions, albeit modified by the CTF. (This may seem obvious, but has nevertheless been the subject of some debate over the years.)

In the 42μm tube data, we see broken pseudo-crystalline Bragg planes in some orientations of the specimen, as shown in Figure 5a. Are these statistical fluctuations, or do they relate to pseudo-crystalline real structure? In our experiment we know that there is indeed a feature of localised order in the solid object, which is here seen in projection, albeit masked by disordered volumes of matter within the same line of sight. The KGH paper reported an extremely clever experiment to distinguish real structure in the image from purely random structure that the eye might wrongly interpret as fringy pseudo Bragg planes. The idea was to scramble the phase of the Fourier transform of the image, and then transform back to the image plane. The phase of each point in the Fourier transform of the image was allocated a random value between 0 and 2π. Any real structure in the original image is therefore destroyed, however the power spectrum of the image is preserved. The reasoning was that if the two images (pre- and post-scrambling) are qualitatively identical, then the original image did not contain any significant structure. KGH tested the method on amorphous silica, a-Ge and a-C, and concluded that only the a-C image was more structured than a purely random fringy image.

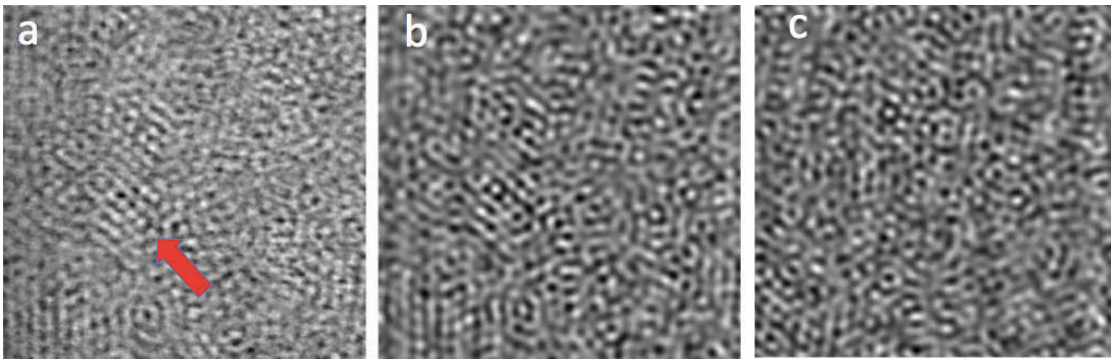

Figure 5: (a) Phase of ptychographic reconstruction. (b) Simulated bright field image of (a). (c) Phase scrambled image from (b). See text for details. The red pointer highlights an area of pseudo-order.

We emulate the experiment here using our X-ray ptychography data. First, we scale the strength of the X-ray ptychographical phase (which varies within the field of view of Figure 2 by 0.9π) by a factor of 0.1 to make it appear a weak phase image. Note that ptycho-tomography can handle strong phase, including multiple phase wraps[17]: here, we are just using the structure of the image to model the weak phase electron image. We then Fourier transform the (complex – weak phase) ptychographic image, multiply it by the transfer function of the objective lens, transform back and then form intensity, giving the bright-field image shown in Figure 5b. Figure 6 shows the diffractogram (Fourier transform of this intensity image) of our modelled bright-field image, fitted as accurately as possible to correspond to the KGH paper. Note that ptychography does not have an equivalent of a contrast transfer function, because, unlike the bright-field

image, there is no requirement to interfere the scattered complex image wave with the unscattered wave. The transfer function in ptychography is near perfect for both modulus and phase components of the image [18].

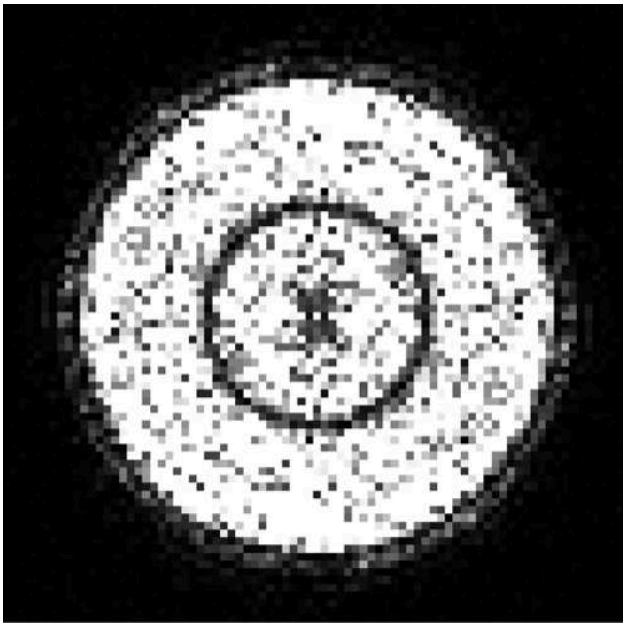

Figure 6: Diffractogram calculated from Figure 5b (the bright-field image). The dark ring is a zero crossing point in the transfer function, which was necessary in the KGH paper so that the second broad transfer region could capture the 3.4 Å fringes from the a-C: compare Figure 4 in KGH [10].

Values of Cs and keV are not reported by KGH, and are not critical to the main argument, provided the transfer function embraces the periodicity of the relevant fringes. Krivanek (private communication) recalls that he used a Siemens 102, at 125 keV, which had a Cs of 2.4mm. The microscope was run to obtain a broad second transfer interval: with this lens (extremely poor by today's standards) it was not possible to reach the 3.4 Å graphite fringe resolution at conventional Scherzer defocus, hence the cross-over in the CTF, leading to the ring of zero transfer in the diffractogram: compare with Figure 4 in KGH [10]. Our glass balls do not have graphite-like structure, but what we can do is to scale the computational experiment so that the Bragg planes caused by the pseudo-crystalline close packing of the glass beads are equivalent to the 3.4 Å planes. Note that the second broad transfer region extends to a reciprocal resolution of 3.1 Å at the second generalised Scherzer defocus, thus allowing the graphite fringes to be visible. We have suppressed high frequency oscillations in the transfer function using a coherence envelope function that renders the width of Fig 6 the same as Figure 4 in KGH.

In the simulated bright-field image, Figure 5b, the very high-frequency information has been lost, but the dominant fringes are expressed almost identically, except for a reversal of contrast (as we would expect given the zero in the CTF). Finally, we show the phase-scrambled image in Fig 5c, which does indeed appear to be significantly more random than Fig. 5b. However, there are

some regions occurring in different locations that do show a small amount of pseudo order on a smaller scale, presumably due to random coincidences of the Fourier components in the image.

We note that in the original KGH paper, the phase scrambling was achieved on the optical bench by using a lens to image the original micrograph onto a second photographic plate. To introduce the random phase, a piece of glass sprayed with lacquer was placed in the back focal plane of the lens. It had a hole in the middle to let through the unscattered beam, which we have also modelled in this calculation. We are grateful to Ondrej Krivanek for pointing out to us that the scale of the random phase variations must be chosen so that the convolution kernel of the randomisation in real space is not too large with respect to the field of view.

In Figure 7a-7c we repeat the same experiment using data from the 117μm diameter tube. The image is taken from one edge of the tube (hence the large-scale darkened contrast on the right of the field of view where the tube is thinner and the associated image phase is smaller). There is clearly some ordering of the glass beads in this thinner area where they are constrained by the tube wall. This structure is once again destroyed by the phase scrambling process, although some very large scale vertical artefacts have been introduced due to residual low frequencies that define the dark edge on the right hand side of Fig 7a. In general, there are rather fewer instances of ordered fringes, even though close examination of Figure 4 shows that there are ordered regions in the specimen. This is because of the projection effect that averages structure as seen through a thicker specimen.

So what does all this show? The main difference from KGH is that here we have no doubt at all that our 'amorphous' object does indeed have three-dimensional regions of order within it, and that this order does manifest itself in the bright-field image despite the projection effect, at least for a thin region of the specimen. Furthermore, this order can indeed be reliably detected using the phase scrambling method. Even with the rather poor imaging capability of microscope used by KGH, we can conclude that it is indeed possible to see indirect evidence of real structure in amorphous carbon.

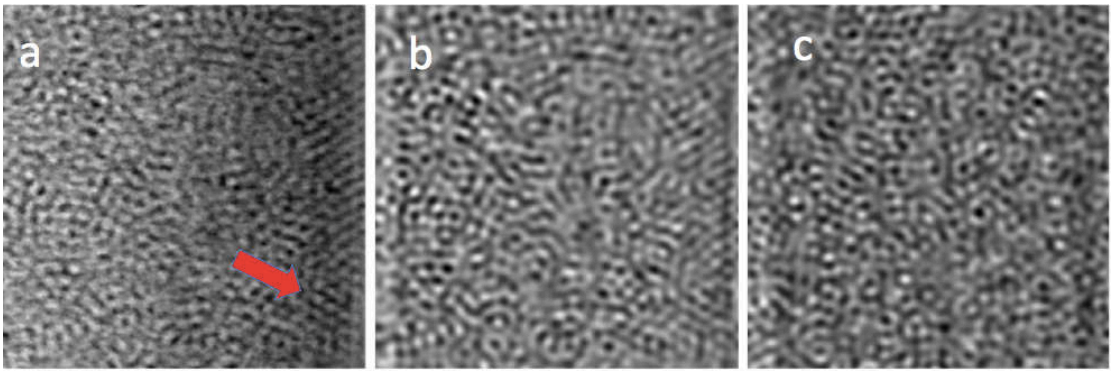

Figure 7: The same series images as Figure 5, but this time taken from the larger 117μm tube. See text for a detail interpretation. The red pointer highlights an area of pseudo-order.

4) Stereoscopic and tomographic imaging of amorphous structure

Elegant though it is, the KGH method does not tell us the exact structure of a disordered specimen. In this section we are going to use our X-ray data to illustrate exactly how demanding it is to infer anything about the 3D structure of a substantially disordered specimen without undertaking a full, computational tomographic reconstruction.

In the 1970s, stereoscopic imaging was a commonly employed technique. Long before tomography, it was seen as an effective way of obtaining depth information, avoiding the projection effect. The human brain is extraordinary adept at processing two images taken from different angles. As alluded to above, there was some hope that combining stereoscopic pairs of images would resolve the amorphous structure problem. Stereoscopic depth resolution relies on the specimen being sparse, for example consisting of distinct particles or simple features separated by a smooth continuum (or empty space). If atoms were point scatterers, then their relative displacement in two stereographic images should allow their 3D position to be plotted, in a way analogous to the astronomers' use of parallax to plot nearby star positions. However, atoms are not very localised points – the atomic potential, which produces bright-field image contrast, is relatively smooth at this resolution. The glass beads in our X-ray experiment are solid balls, which also do not very accurately model the atomic potential, but they are probably more like the apparent shape of atoms at the resolution of the original experiment (about 3Å) than isolated point scatterers, because of the convolution with the point spread function of the lens. This model allows us to see what the stereoscopic image of our model system would look like, given the resolution available in the 1970s.

In Figure 8 can be viewed as two stereoscopic pairs of the 42μm tube X-ray ptychographic data. The two images at the top are separated by a 1 degree tilt angle, the two images at the bottom are separated by a 2 degrees tilt angle. These can be viewed as stereograms by the naked eye if the reader has some patience. The trick is to cross your eyes until the large pointers from the two images align with one another. There will now be three large pointers and three images visible, but make every effort to concentrate only on the central, overlapped image. If the pointers are vertically displaced from one another, tilt your head sideways to bring them into alignment. Now very carefully look into the fringy images, perhaps using the smaller pointers as additional aids to fix upon.

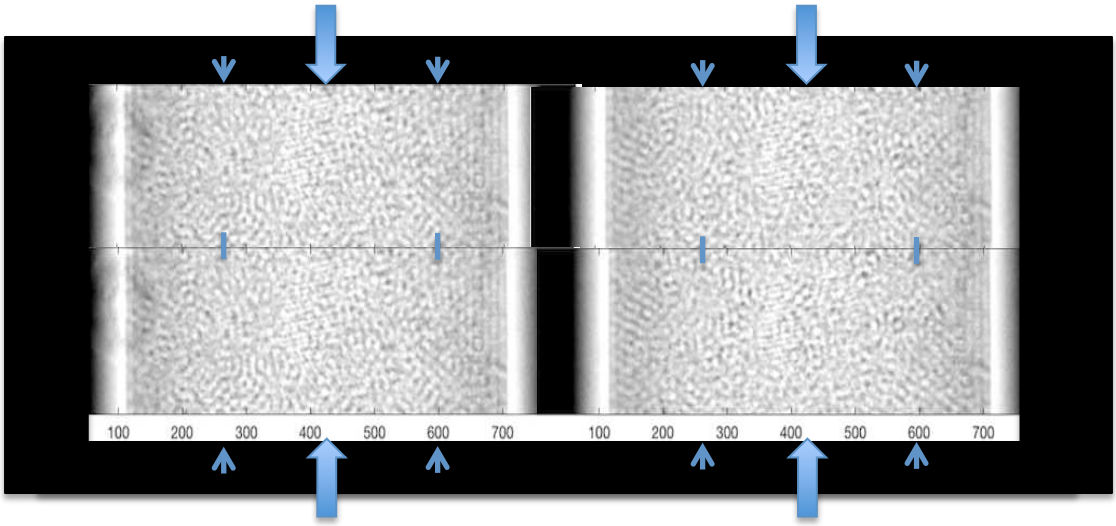

Figure 8) Stereographic pairs of images taken from the 42μm tube data. The two images on the left are identical phase images from one projection of the ptychographical data. The top right image is the phase image from an angle rotated by one degree from the left image. The bottom right image is rotated by two degrees. The images are laterally compressed to enhance the 3D effect. See main text for how to view the stereogram.

It is hard, but if you take your time you should now be able to see multiple layers in the specimen. A crystallite is very clearly visible, hanging at the front of the object space and in the middle of the field of view. The 2 degree data is more strikingly 3D, but is also more confusing. At this amount of tilt, beads at the top and bottom surfaces of the tube have moved by a whole bead diameter relative to one another, so it is harder to unambiguously estimate the depth information. Readers may alternatively cut and paste these images into a smart phone app that can be used with stereoscopic lenses, such as Google Cardboard.

In the supplementary data on-line, we present full rotational tomographic movies of both the 42μm and 117μm tube data, showing consecutive tilts separated by 2 degrees. In the 42μm data, the rotational motion is very clear, especially near the edges of the sample, but is rather more confused in the central, thick area of the sample. For the 117μm specimen, rotation is also very clear at the edge of the sample (especially on the left hand side, between 40 and 70 degrees, where there is a crack in the bead structure). However, it is impossible to perceive any systematic rotational motion of correlation in the beads in the central region of the specimen. If scaled to an electron experiment, the diameter of the tube would be about 250A – in other words, thick. No single projection correlates to the next projection. The fringy structure of the images between consecutive projections changes completely.

We already know that when all of these images are put together in a back-projection tomographic reconstruction, we see the beads very clearly: all the 3D information is in these data, but it cannot be extracted by simple parallax. Furthermore, each projection appears as equally random as any other projection. In short, any single fringy image, or pair of stereoscopic images, in most cases tells us very little about the 3D structure, notwithstanding the measure of

significant local order made by the KGH technique in the previous section and similar statistical techniques such as fluctuation microscopy.

5) Discussion and conclusions

We have modelled the challenge of imaging amorphous materials in the electron microscope using X-ray ptychography. By up-scaling the dimensions of the atoms to 1μm diameter glass beads, X-ray ptycho-tomography can easily obtain an explicit three-dimension reconstruction of a substantially amorphous specimen that contains some small volumes of local ordering. Using this, we can see that the sort of fringy images that are so often seen in the electron microscope from amorphous specimens are generated by the exact atomic positions, and are not simply an artefact of the transfer characteristics of the lens. Furthermore, we can correlate 3D order in the object with the appearance of semi-ordered fringes in the image, and that this structure can be reliably distinguished by a simple Fourier phase scrambling technique developed over 40 years ago. By looking a set of projections from our model, we can see that any attempt to process either a single image or a pair of stereographic images in order to determine the exact structure of the object is futile.

These conclusions are not particularly surprising, but the visual impact of the results, especially the rotational tomography movies, do serve to illustrate the extremely data-intensive nature of mapping hundreds of thousands of atoms in an amorphous structure. The only hope of doing so is to undertake a fully-fledged tomographic reconstruction.

Of course, doing this experiment for real with electrons looking at atoms would be much harder than our X-ray equivalent. We would have to deal with specimen damage, contamination, and – perhaps worst of all – dynamical scattering effects (although these are less pathological for amorphous structures than for crystals). Rather than relying on the bright-field or ADF image, we would propose that the best signal to employ would be the electron ptychographical image: this reconstructs strong phase contrast accurately with minimal dose, it is not limited by the lens resolution and so 'softer' low-energy electrons can be employed, minimising knock-on damage [19, 20], at least for some specimens. The phase signal is cumulative and linear and so it is ideal for tomography, as is well documented in the X-ray ptychography literature [17, 21]. It is also known that multiple scattering effects can be removed from a comprehensive ptychography data set [22], and anyway electron ptychography is rather less sensitive to dynamical scattering than the conventional exit wave, even in the case of strongly scattering periodic structures[23]. With regard to damage, we note that the total number of X-ray counts we recorded for our tomographic reconstructions (i.e. summed over all tomographic projections) would be equivalent to about half hour exposure time within a typical STEM beam. That is quite a lot of dose. However, we made no attempt to minimise our dose and/or optimise our inversion algorithm to use minimal counts, say via maximum likelihood methods [24].

Acknowledgements

This work was funded in part by the Electronic and Electrical Engineering Department of University of Sheffield. PL would like to thank the Chinese Scholarship Council (CSC) for financial support. We thank Diamond Light Source for access to the coherence branch of beamline I13, proposal number MT11877 (Rodenburg), where all the data reported were collected.

Competing interests: JMR retains a 2.86% shareholding in a spin-out company of the University of Sheffield, Phase Focus Ltd, that holds patents relating to ptychography.

Supplementary On-line Data: Movie files

FILE1: 'phase_projection_42um': avi movie file showing the tomographic phase images of the 42μm tube rotating around its axis.

FILE2: 'phase_projection_117um': avi movie file showing the tomographic phase images of the 117μm tube rotating around its axis.

References

1. Howie, A., *HIGH-RESOLUTION ELECTRON-MICROSCOPY OF AMORPHOUS THIN-FILMS.* Journal of Non-Crystalline Solids, 1978. **31**(1-2): p. 41-55.
2. Howie, A., *Application of electron optical techniques to the study of amorphous materials.* Philosophical Magazine, 2010. **90**(35-36): p. 4647-4660.
3. PB Hirsch, A.H., RB Nicholson, DW Pashley and MJ Whelan, *Electron microscopy of thin crystals*. 1965: Butterworth.
4. Gaskell, P.H. and D.J. Wallis, *Medium-range order in silica, the canonical network glass.* Physical Review Letters, 1996. **76**(1): p. 66-69.
5. Mountjoy, G., *Atomic structure of amorphous solids from high resolution electron microscopy - a technique for the new millennium?* Journal of Non-Crystalline Solids, 2001. **293**: p. 458-463.
6. Alben, R., G.S. Cargill and J. Wenzel, *ANISOTROPY OF STRUCTURAL MODELS FOR AMORPHOUS MATERIALS.* Physical Review B, 1976. **13**(2): p. 835-842.
7. Dierolf, M., A. Menzel, P. Thibault, P. Schneider, C.M. Kewish, R. Wepf, O. Bunk and F. Pfeiffer, *Ptychographic X-ray computed tomography at the nanoscale.* Nature, 2010. **467**(7314): p. 436-U82.
8. Rodenburg, J., A. Hurst and A. Cullis, *Transmission microscopy without lenses for objects of unlimited size.* Ultramicroscopy, 2007. **107**(2): p. 227-231.
9. Maiden, J.R.a.A., *Ptychography.* Handbook of Microscopy, 2019.
10. Krivanek, O.L., P.H. Gaskell and A. Howie, *SEEING ORDER IN AMORPHOUS MATERIALS.* Nature, 1976. **262**(5568): p. 454-457.
11. Treacy, M.M.J., J.M. Gibson, L. Fan, D.J. Paterson and I. McNulty, *Fluctuation microscopy: a probe of medium range order.* Reports on Progress in Physics, 2005. **68**(12): p. 2899-2944.
12. Gibson, J.M., M.M.J. Treacy and P.M. Voyles, *Atom pair persistence in disordered materials from fluctuation microscopy.* Ultramicroscopy, 2000. **83**(3-4): p. 169-178.
13. Gibson, J.M. and M.M.J. Treacy, *Diminished medium-range order observed in annealed amorphous germanium.* Physical Review Letters, 1997. **78**(6): p. 1074-1077.
14. Maiden, A.M. and J.M. Rodenburg, *An improved ptychographical phase retrieval algorithm for diffractive imaging.* Ultramicroscopy, 2009. **109**(10): p. 1256-1262.
15. Li, P., *Investigations and improvements in ptychographic imaging*, in *Electronic and Electrical Engineering*. 2016, University of Sheffield: White Rose eTheses online.
16. Barrett, J.F. and N. Keat, *Artifacts in CT: Recognition and avoidance.* Radiographics, 2004. **24**(6): p. 1679-1691.
17. Diaz, A., P. Trtik, M. Guizar-Sicairos, A. Menzel, P. Thibault and O. Bunk, *Quantitative x-ray phase nanotomography.* Physical Review B, 2012. **85**(2).

18. Godden, T.M., A. Muniz-Piniella, J.D. Claverley, A. Yacoot and M.J. Humphry, *Phase calibration target for quantitative phase imaging with ptychography.* Optics Express, 2016. **24**(7): p. 7679-7692.
19. Jiang, Y., Z. Chen, Y. Hang, P. Deb, H. Gao, S. Xie, P. Purohit, M.W. Tate, J. Park, S.M. Gruner, V. Elser and D.A. Muller, *Electron ptychography of 2D materials to deep sub-angstrom resolution.* Nature, 2018. **559**(7714): p. 343-+.
20. Rodenburg, J., *A record-breaking microscope.* Nature, 2018. **559**: p. 334-335.
21. Pfeiffer, F., *X-ray ptychography.* Nature Photonics, 2018. **12**(1): p. 9-17.
22. Maiden, A.M., M.J. Humphry and J. Rodenburg, *Ptychographic transmission microscopy in three dimensions using a multi-slice approach.* JOSA A, 2012. **29**(8): p. 1606-1614.
23. Plamann, T. and J. Rodenburg, *Electron ptychography. II. Theory of three-dimensional propagation effects.* Acta Crystallographica Section A: Foundations of Crystallography, 1998. **54**(1): p. 61-73.
24. Thibault, P. and M. Guizar-Sicairos, *Maximum-likelihood refinement for coherent diffractive imaging.* New Journal of Physics, 2012. **14**.